Alginate-lignin Bonded *Rhizophora* spp. Particleboard as a Natural-based Tissue-equivalent Phantom

Saadiatul Nur Aqilah Mohd Zakaria,[a] Siti Hajar Zuber,[a,f,*] Mohd Hafiidz Jaafar,[b] Muhammad Safwan Ahmad Fadzil,[a] Wan Nordiana W. Abd Rahman,[c] Mohd Zahri Abdul Aziz,[d] Abd Aziz Tajuddin,[e] Seán B. Leen,[f] and Pouyan Ghabezi [f]

Experimental particleboards were fabricated using *Rhizophora* spp. wood trunks, incorporating three different percentages of lignin and sodium alginate (0%, 3%, and 6%) as adhesives, as well as three different sample sizes of *Rhizophora* spp.: 0 to 104 μm, 105 to 210 μm, and 211 to 500 μm. The objective was to investigate the physical, morphology, chemical composition, and effective atomic number Z_{eff} of *Rhizophora* spp. particleboards incorporated with lignin and sodium alginate. The physical properties were studied using gravimetric method, thickness swelling, and water absorption tests. The fabricated particleboards had a suitable physical and radiological characteristic for tissue-equivalent phantom applications. The reduction in particle size and increase in adhesive content contributed to lower thickness swelling and water absorption. The density values fell within the specified range. According to scanning electron microscopy observations, increased adhesive content decreased the formation of voids in the structure of particleboards. The calculated effective atomic number further supported the suitability of material. Higher sodium alginate usage was found to be associated with an increase in sodium content. The sample A_6 with a particle size of 0 to 104 μm and 6% adhesive exhibited promising suitability for the fabrication of tissue-equivalent phantom.

DOI: 10.15376/biores.21.3.8444-8466

Keywords: Rhizophora spp.; Particleboard; Physical properties; Morphology study; Alginate-lignin adhesive

*Contact information: a: Faculty of Health Sciences, Universiti Kebangsaan Malaysia, 50300, Kuala Lumpur, Malaysia; b: School of Industrial Technology, Universiti Sains Malaysia, 11800, Penang, Malaysia; c: Faculty of Science and Technology, Universiti Kebangsaan Malaysia, 43600, Selangor, Malaysia; d: Pusat Perubatan USM, Universiti Sains Malaysia, 13200, Pulau Pinang, Malaysia; e: Albukhary International University, 05200, Kedah, Malaysia; f: School of Engineering, University of Galway, H91 TK33, Galway, Ireland; *Corresponding author: hajarzuber@ukm.edu.my*

INTRODUCTION

A phantom is a test specimen used in medical imaging to replicate biological tissue by mimicking the structural characteristics and relevant physical properties of the original clinical object. There are numerous types of phantoms that are designed to fulfill specific functions ranging from calibration and quality control to educational purposes (Wegner *et al.* 2023). According to a previous study (Khallouqi *et al.* 2024), dosimetry cannot be performed on human subjects because of ethical and practical constraints. Consequently, the development of materials that can replicate the physical characteristics of human tissues and organs in computed tomography scans is necessary. A primary obstacle in the process of creating phantoms is identifying appropriate materials that correspond to the essential physical characteristics of human tissues, including mass attenuation coefficient, Computed Tomography (CT) number, effective atomic number, electronic density, and physical density. For example, water is frequently used as a reference material for soft tissue but has problems with contamination, evaporation, leakage, and temperature dependence (Karthikeyan and Samual 2022; Khallouqi *et al.* 2024). When using anthropomorphic phantoms in diagnostic radiology and radiotherapy, all structures must be able to accurately replicate the intended patient geometries, offer sufficient tissue equivalents, and be sensitive to radiation effects (Jusufbegović *et al.* 2022).

Although anthropomorphic phantoms constructed from tissue-equivalent materials are costly, ongoing research into alternative materials has shown progress in developing more cost-effective phantoms, reducing fabrication time, and facilitating disease-related research. For example, a mixture of paraffin wax and sodium chloride, a common salt, has been suggested as a substitute material for soft tissue (Bello *et al.* 2022). Phantoms are often fabricated from biological materials, such as vegetables, or gelatinous substances embedded with conductive particles, however, these materials often exhibit poor mechanical properties and reduced stability. Incorporating materials such as silicones, elastomers, and filled polymers can significantly enhance both mechanical performance and long-term durability (Bublex *et al.* 2025). Water is used universally in radiotherapy and has been recognized by the International Atomic Energy Agency (IAEA) as a standard phantom (Zuber *et al.* 2021c). However, several commercially available phantoms, such as those made of polystyrene, acrylic, and wood, have replaced water for dosimetry studies because of their physical properties and solid-like form. The ATOM ® phantom (CIRS, Norfolk, VA) and the RANDO phantom (Alderson Research Labs, Stanford, CA) are two readily available but expensive anthropomorphic phantoms that are frequently used for radiation studies.

Polymethyl methacrylate (PMMA) has been extensively employed as a tissue-equivalent phantom material due to its attenuation properties, which closely resemble those of water and soft tissue within computed tomography (CT) energy ranges. However, despite its favorable radiological properties, the application of PMMA is often constrained by its relatively high fabrication cost, particularly in regions with limited access to medical imaging resources (Khallouqi *et al.* 2025). In addition, although PMMA exhibits biocompatibility and recyclability, it remains a non-biodegradable polymer, and its recycling processes may generate environmentally hazardous by-products (Zuber *et al.* 2021a). Previous studies on phantom fabrication have investigated various materials to simulate the properties of human tissue, including beeswax as a soft tissue substitute. Nevertheless, the application of beeswax is limited by its relatively low melting point and poor mechanical stability. In particular, its tendency to become brittle at low temperatures may adversely affect structural integrity, thereby limiting its long-term durability and suitability for phantom application (Nisa *et al.* 2025).

Overall, these limitations highlight the necessity for developing alternative materials, such as a combination of sodium alginate, lignin, and *Rhizophora* spp., which are expected to offer adequate radiological performance while also providing advantages in terms of cost efficiency, mechanical stability, and environmental sustainability.

Rhizophora spp. refers to several species of *Rhizophora*, a genus of tropical mangrove trees characterized by their adaptability to environmental fluctuations and typical growth within tidal zones. Subsequent investigations have explored the use of *Rhizophora* spp. as a tissue-equivalent material. Due to its tendency to warp and crack over time, *Rhizophora* spp. was processed into particleboards, resulting in improved volumetric uniformity (Zuber *et al.* 2021b). *Rhizophora* spp. are commonly used as fuelwood or charcoal and serve as raw materials in the synthetic, chipboard, and pulpwood industries. Additionally, *Rhizophora* spp. has been shown to function effectively as a phantom material that simulates human soft tissue. The attenuation properties of *Rhizophora* spp. wood exhibits closer similarity to the attenuation outcomes for water compared to many other materials classified as tissue-equivalent (Zuber *et al.* 2020a). *Rhizophora* spp. offers numerous advantages, including low cost, non-toxicity, high thermal stability, biodegradability, and radiation and dosimetric properties comparable to those of water (Samson *et al.* 2025). According to previous study (Abuarra *et al.* 2014), when raw wood is ground into tiny particles and compressed into particleboards, the attenuation properties are improved, additional materials can be added to improve the mechanical and physical features of the particleboards, and it will be easier to create tissue-equivalent phantoms in the required size, density, and shape.

Lignin constitutes approximately 15 to 30% of the total lignocellulosic biomass of plants and trees. Lignin is recognized as the second most abundant natural biopolymer on Earth (Shah *et al.* 2023; Ali *et al.* 2024). It is the predominant non-carbohydrate component responsible for imparting rigidity and hydrophobicity to plant cell walls (Wu *et al.* 2023; Ali *et al.* 2024). Lignin exhibits strong affinity toward cellulose and hemicellulose, possessing a complex aromatic heteropolymer structure (Ali *et al.* 2024). In wood, lignin functions as a sort of "glue" and shields trees from UV rays. Because lignin contains a comparatively high amount of carbon, approximately 60 to 65%, it is considered to be an effective raw material for carbon fiber because it yields a significant amount of carbon (Peijs *et al.* 2022). Lignin is a natural, renewable, and amphiphilic polymer derived from the hydroxycinnamyl alcohols p-coumaryl, coniferyl, and sinapyl. It has been widely reported that lignin possesses desirable properties for both environmental and industrial applications, such as a high degree of functionality, improved adhesion, adsorption, and solution characteristics, as well as good biocompatibility, low toxicity, and antibacterial activity (Linan *et al.* 2024).

Sodium alginate is an anionic, linear polysaccharide composed of repeating units of D-mannuronic acid and L-guluronic acid residues linked by 1-4 glycosidic bonds (Badita *et al.* 2020; Akbar *et al.* 2023; Qiu *et al.* 2024). Sodium alginate is derived from seawater brown algae, where it is primarily located in the outer cell wall layer. Sodium alginate exhibits numerous advantageous properties, including pH sensitivity, non-toxicity, biodegradability, perishability, safety, non-immunogenicity, linearity, hydrophilicity, poly-anionic character, cost-effective adhesive capability, and excellent biocompatibility (Akbar *et al.* 2023). Sodium alginate is extensively employed as a thickening agent, stabilizer, and adhesive in a variety of industries, including food packaging and cosmetics, because of its superior film-forming capability, excellent thickening properties, and biodegradable nature (Luan *et al.* 2025). Alginate needs to be highly pure and safe for the body to be utilized in the pharmaceutical and biomedical industries (Frent *et al.* 2022).

Alternatively, previous studies have demonstrated the potential of bio-based adhesives, including soy protein, tannin, starch, lignin, animal glue, and natural rubber, for the fabrication of *Rhizophora* spp. particleboards. The increasing interest in these materials is primarily driven by environmental and health concerns associated with formaldehyde-based adhesives. However, unmodified soy protein has been reported to exhibit limited adhesive performance due to its sensitivity to variations in temperature, pH, viscosity, ionic strength, and stress conditions. In addition, its poor mechanical and dimensional stability further restricts its applicability as an effective bonding agent (Samson *et al.* 2020b). Similarly, starch-based adhesives remain largely limited to laboratory-scale applications and have not been extensively commercialized in industrial production. This limitation is primarily attributed to their poor water resistance, low bonding strength, and variability in physicochemical properties arising from differences in the growth conditions of starch sources (Maulana *et al.* 2022). In contrast, alginate and lignin have attracted considerable attention owing to their diverse biological functionalities, including anticancer, antibacterial, and antioxidant properties. Furthermore, these biopolymers have been reported to enhance mechanical performance, improve water-retention capacity, and provide effective ultraviolet (UV) resistance (Hoan *et al.* 2023).

The present study utilized lignin and sodium alginate as adhesive materials in the fabrication of *Rhizophora* spp. particleboard with varying adhesive percentages to produce a tissue-equivalent material. The physical properties of particleboard were studied through density determination by gravimetric method, thickness swelling, and weight absorption test. The morphology study, elemental composition, and effective atomic number were performed for all the alginate-lignin bonded *Rhizophora* spp. particleboards.

EXPERIMENTAL

Fabrication of Particleboard from Alginate-lignin Bonded *Rhizophora* spp.

Rhizophora spp. was collected from a mangrove factory in Klang, Selangor, and Kuala Sepetang, Perak. Lignin and sodium alginate in powder form were purchased from Macklin (Shanghai Macklin Biochemical, Shanghai, China). The wood trunks were first dried and then cut into a smaller size using a JWBS-14Q band saw (JET, USA). Subsequently, that wood was milled into a smaller particle size using a grinder machine (Retsch, Germany). The wood with smaller particle size was first dried before being sieved using a sieve machine. Finally, *Rhizophora* spp. powder with different particle sizes, 0 to 104 μm, 105 to 210 μm, and 211 to 500 μm was collected and then dried prior to the fabrication of the particleboards. In this study, *Rhizophora* spp. particle sizes of 0 to 104 μm, 105 to 210 μm, and 211 to 500 μm were selected. Smaller particle sizes are associated with reduced void spaces and enhanced particle bonding within the matrix. The decrease in void content contributes to improve structural compaction and produce in a smoother surface morphology compared to larger particle sizes (Marashdeh *et al.* 2011; Tousi *et al.* 2015).

Experimental particleboards were fabricated using *Rhizophora* spp. wood incorporating three different percentages of lignin and sodium alginate, 0%, 3% (2.5% sodium alginate and 0.5% lignin), and 6% (5% sodium alginate and 1% lignin) as an adhesive mixture. Previous study has reported the development of phantom materials based on *Rhizophora* spp. particleboards bonded with soy flour and lignin as adhesives at 0%, 6%, and 12% (Zuber *et al.* 2024). However, the 12% adhesive formulation was not preferred for further consideration due to poorer uniformity and homogeneity. Based on these findings, this study selected 0%, 3%, and 6% adhesive formulations to evaluate their effects on physical and radiological properties. The 0% adhesive served as a control sample, while 3% and 6% adhesive represented low and previously identified optimal adhesive formulations for phantom material applications. Table 1 records the particle sizes and adhesive content for each sample.

Table 1. Particle Sizes and Adhesive Content for Each Sample

Sample	Particle Size (μm)	Adhesive Content (%)
A_0	0-104	0% Sodium alginate and Lignin
A_3	0-104	2.5% Sodium alginate and 0.5% Lignin
A_6	0-104	5% Sodium alginate and 1% Lignin
B_0	105-210	0% Sodium alginate and Lignin
B_3	105-210	2.5% Sodium alginate and 0.5% Lignin
B_6	105-210	5% Sodium alginate and 1% Lignin
C_0	211-500	0% Sodium alginate and Lignin
C_3	211-500	2.5% Sodium alginate and 0.5% Lignin
C_6	211-500	5% Sodium alginate and 1% Lignin

Prior to particleboard fabrication, the raw materials comprising *Rhizophora* spp., lignin, and sodium alginate powders were subjected to thermogravimetric analysis (TGA) to evaluate their thermal stability and determine the appropriate hot-pressing temperature for particleboard production. The moisture content of the raw materials was determined using a digital moisture analyzer (Shimadzu, Japan). The raw materials were required to exhibit a moisture content less than 10%. The moisture content of the raw materials is presented in Table 2 and were subsequently used in the calculations described in Eq.1,

Table 2. Moisture Content of the Raw Materials

Sample	Particle Size (μm)	Moisture Content of *Rhizophora* spp. (%)	Moisture Content of Sodium Alginate (%)	Moisture Content of Lignin (%)
A	0 to 104	6.95	6.73	9.06
B	105 to 210	6.97	6.55	9.67
C	211 to 500	6.98	6.73	9.15

The *Rhizophora* spp. powder, sodium alginate, and lignin were thoroughly mixed to create a homogenous mixture. The mixture was placed into a customized mould and compressed for 3 min to form particleboards without air gap. The particleboards were prepared using hot-pressing at approximately 200 °C, with pressure of 20 MPa for about 20 min. The dimension of particleboards was (23 × 23 × 0.5) cm^3. Then, the particleboards underwent a cold compression for approximately 10 min. The particleboards were fabricated with a target density of 1.0 gcm^{-3}. The proportions of *Rhizophora* spp. powder, adhesive materials, and water used in the fabrication of the particleboards were calculated in accordance with previous studies (Tousi *et al.* 2014) and defined by Eq. 1,

$$\rho = \frac{M}{V}; \rho_t = 1\ \text{gcm}^{-3}$$
$$M_R = W_R\% \times \rho V \times (1 + MC\%_R)$$
$$M_A = W_A\% \times \rho V \times (1 + MC\%_A)$$
$$M_L = W_L\% \times \rho V \times (1 + MC\%_L)$$
$$M_W = 7\% \times \rho V - [(M_R \times MC\%_R) + (M_A \times MC\%_A) + (M_L \times MC\%_L)] \quad (1)$$

where ρ, ρ_t, M, and V are density (gcm^{-3}), target density (gcm^{-3}), mass (g), and volume (cm^3) of the particleboard, respectively. Parameters M_R, $W_R\%$, and $MC\%_R$ are the approximate mass (g), weight percentage (%), and moisture content (%L) of *Rhizophora* spp. Powder, respectively. The parameters M_A, $W_A\%$, and $MC\%_A$ are the approximate mass (g), weight percentage (%), and moisture content (%L) of sodium alginate. Parameters M_L, $W_L\%$, and $MC\%_L$ are the approximate mass (g), weight percentage (%), and moisture content (%L) of lignin. Parameter M_W, is the approximate mass (g) of saline water.

Thermal Stability Using Thermogravimetric Analysis

Thermogravimetric analysis (TGA) was carried out with a device from Linseis (Germany) to determine the thermal decomposition behavior of the *Rhizophora* spp., sodium alginate, and lignin. The study was carried out at the Earth Material-Characterization laboratory in the Center of Global Archeological Research, Universiti Sains Malaysia. A 0.5 g portion of each raw material in powdered form was prepared for the analysis. The measurements were recorded in the range temperatures between 30 ℃ and 800 ℃ with a heating rate at 10 ℃/min under a nitrogen atmosphere.

Density Determination by Gravimetric Method

The density of each particleboard sample was determined using the gravimetric method, based on precise measurements of its external dimensions. The samples of the particleboards were prepared in the size of (3.0 × 3.0 × 0.5) cm^3 using a saw machine. For the gravimetric method, a digital caliper was used to measure the thickness, length, and width of each particleboard sample. An electronic balance was used to measure the mass of each particleboard sample. The density of the particleboard samples was calculated by Eq. 2:

$$Density\ (gcm^{-3}) = \frac{Mass\ (g)}{Volume\ (cm^3)} \quad (2)$$

The density calculation did not account for internal air voids within the particleboard, which may have influenced the measured density values. The density of each particleboard was measured and recorded.

Water Absorption and Thickness Swelling Test

The dimensional stability of particleboard samples was determined using water absorption (WA) and thickness swelling (TS) tests according to Japanese Industrial Standard, JIS A-5908 (JIS A 5908 2003) for particleboard. The dimension of particleboard samples was prepared in the size of (2.0 × 2.0 × 0.5) cm^3. For the WA test, the weight of each sample was measured using an electronic balance and recorded as pre immersion in water (W_0). Each sample was immersed in distilled water for 24 h. After 24 h, each sample was removed from the water, and the excess water wiped off. The weight of each sample was measured and recorded as post immersion in water (W_{24}).

For TS test, the thickness of each sample was measured using a digital caliper and recorded as pre immersion in water (t_0). Each sample was immersed in distilled water for 24 h. After 24 h, each sample was removed from the water, and the excess water wiped off. The thickness of each sample was measured and recorded as post immersion in water (t_{24}). The results of WA and TS tests are presented in Fig. 1. The tests were calculated by Eqs. 3 and 4,

$$Water\ absorption\ (\%) = \frac{W_{24} - W_0}{W_0} \times 100\% \quad (3)$$

where W_0 and W_{24} are the average weight (g) of the sample before and after 24 h immersion in water. Thickness swelling was calculated using Eq. 4,

$$Thickness\ swelling\ (\%) = \frac{t_{24} - t_0}{t_0} \times 100\% \quad (4)$$

where t_0 and t_{24} are the average thickness (cm) of the sample before and after 24 h immersion in water.

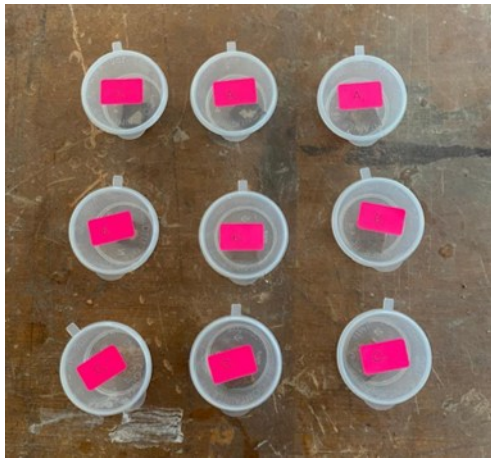

Fig. 1. Preparation of sample for thickness swelling and water absorption test

Morphology Study Using Scanning Electron Microscopy

Scanning Electron Microscopy (SEM) analysis was performed using Field Emission Scanning Electron Microscopy (FESEM) (Supra 55VP, Zeiss) to determine the morphology and elemental information with virtually unlimited depth of field at magnifications ranging from 10× to 300,000×. The study was carried out at the I – CRIM Centralised Lab, Centre for Natural and Physical Laboratory Management UKM (ALAF - UKM), Research Complex Universiti Kebangsaan Malaysia. The samples of particleboards were prepared in the size of (0.5 × 0.5 × 0.5) cm^3. The images were captured with magnification of 1000×, 2000×, and 4000×. FESEM was utilized to analyze insulating samples without the application of conductive coating materials, including carbon, gold, or platinum.

Elemental Composition using Energy Dispersive X-ray

Energy Dispersive X-ray (EDX) analysis was performed to determine the elemental information of the samples. The study was carried out at the I – CRIM Centralised Lab, Centre for Natural and Physical Laboratory Management UKM (ALAF - UKM), Research Complex Universiti Kebangsaan Malaysia. The samples of particleboards were prepared in the size of (0.5 × 0.5 × 0.5) cm^3. The EDX analysis was used to determine the weight percentage of elements in the sample.

Effective Atomic Number, Z_{eff} Using Energy Dispersive X-ray

The EDX analysis was performed to determine the weight percentage of elements in the sample. The Z_{eff} of the particleboard samples was calculated using Eq. 5,

$$Z_{eff} = [\sum_{i=1}^{n}(e_i Z_i^m)]^{(\frac{1}{m})} \quad (5)$$

where e_i and Z_i are electron fraction and atomic number of i^{th}element in the sample, respectively; and m is a fixed value of 3.4, which represents the hypothetical coefficient for water and biological matters. The electron fraction of the i^{th}element can be calculated using Eq. 6,

$$e_i = \frac{w_i(\frac{Z_i}{A_i})}{\sum w_i(\frac{Z_i}{A_i})} \quad (6)$$

where w_i, and A_i are fractional weight and atomic mass of i^{th}element in the sample, respectively.

RESULTS AND DISCUSSION

Thermogravimetric Analysis of Raw Materials

The thermogravimetric analysis (TGA) is a thermal analysis technique used to evaluate the thermal behavior of materials over controlled temperature range. During heating, the material may undergo physical or chemical changes accompanied by heat absorption or release, resulting in variations such as mass loss, decomposition, or changes in material properties (Ahluwalia 2023). Differential scanning calorimetry (DSC) measures heat flow in a material as it is heated or cooled, revealing thermal transitions such as melting and phase changes. It is commonly combined with TGA to provide a more complete thermal characterization (Slobozeanu *et al.* 2021). Figure 2 demonstrates the TGA and DSC curve for the raw materials, *Rhizophora* spp., sodium alginate, and lignin.

Figure 2 presents the TGA and DSC curves demonstrated the thermal degradation behavior of the raw materials over a temperature range of approximately 30 to 800 °C. Initial weight loss observed at lower temperature was attributed to moisture evaporation, followed by the decomposition of hemicellulose and cellulose at elevated temperatures. Hemicellulose degradation occurred at lower temperature due to dehydration, oxidation, carbon dioxide evolution, and the formation of carbonyl and carboxyl groups, whereas cellulose decomposition occurred subsequently with rapid volatilization, producing volatile and flammable compounds (Zuber *et al.* 2020a).

For *Rhizophora* spp., the TGA results showed a total mass loss of approximately 84.0%, with an initial weight loss of 25.5% below 250 °C attributed to moisture evaporation. Major thermal degradation occurred between 250 and 400 °C, which was attributed to the decomposition of organic constituents. The DSC curve revealed a major thermal reaction between 333.3 °C and 345.4 °C, with a peak temperature at 336.9 °C and an enthalpy value of -150.90 J/g, indicating an exothermic degradation process. For sodium alginate, the TGA results showed a total mass loss of approximately 92.38%, with an initial weight loss of 23.19% below 250 °C attributed to moisture evaporation. Major thermal degradation occurred between 250 °C and 350 °C due to the decomposition of organic constituents. The DSC curve revealed a major thermal reaction between 299.4 °C and 329.6 °C, with a peak temperature at 302.7 °C and an enthalpy value of -903.48 J/g, indicating an exothermic degradation process.

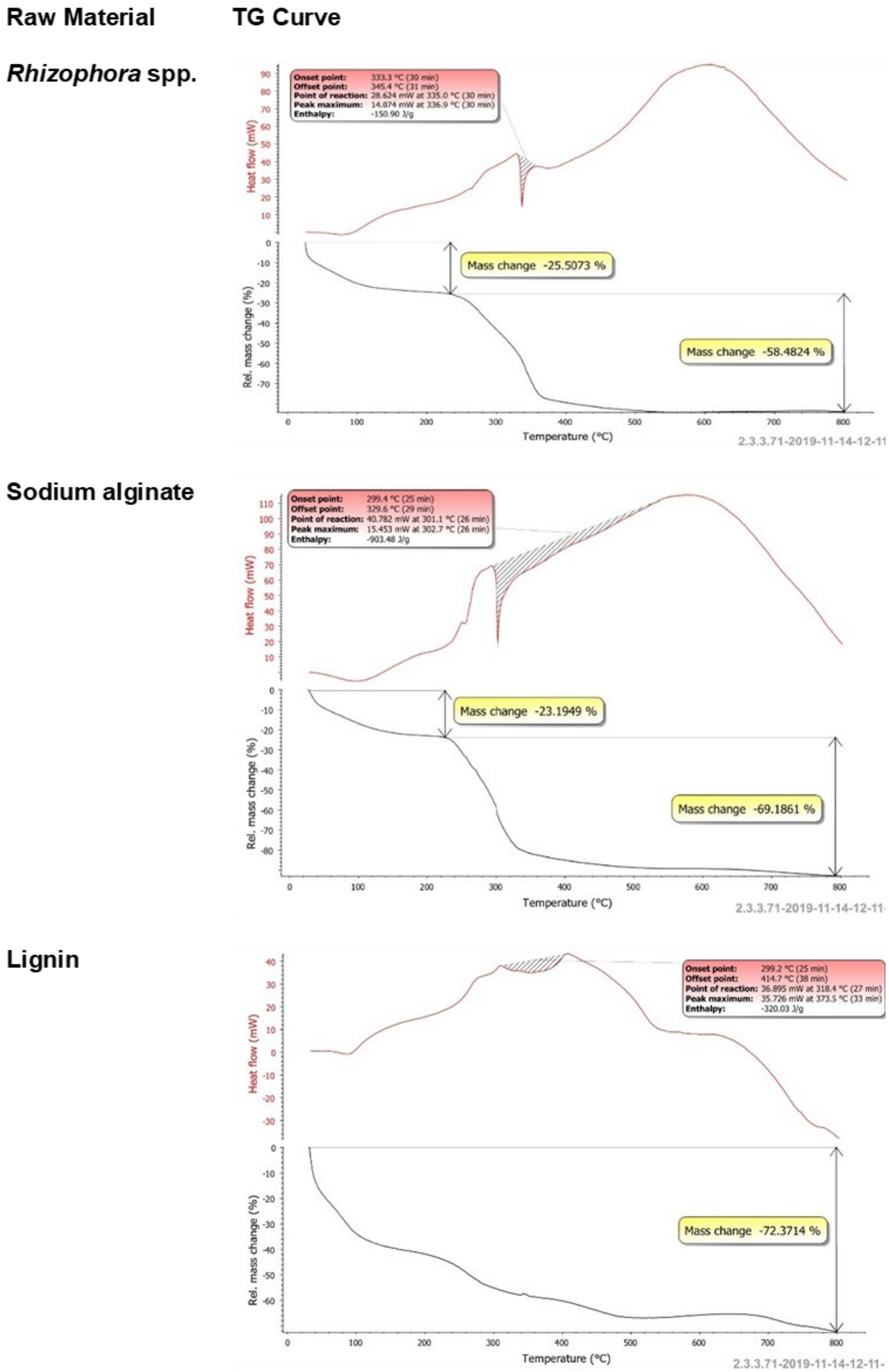

Fig. 2. TGA and DSC curves of Rhizophora spp., sodium alginate, and lignin in the fabrication of particleboard

For lignin, the TGA results showed a total mass loss of 72.4%, with an initial loss below 150 °C attributed to moisture evaporation. Major thermal degradation occurred between 250 and 500 °C due to the decomposition of organic constituents. The DSC curve revealed a major thermal reaction between 299.2 and 414.7 °C, with a peak temperature at 373.5 °C and an enthalpy value of -320.03 J/g, indicating an exothermic degradation process. Based on Fig. 2. the results demonstrate that the raw materials, including *Rhizophora* spp., sodium alginate, and lignin remained thermally stable below 300 °C before significant thermal decomposition occurred. Therefore, the compression temperature employed during the particleboard fabrication process should remain below the thermal degradation temperature to enhance the interfacial bonding efficiency between the fibre chains of *Rhizophora* spp., sodium alginate, and lignin while preventing the thermal decomposition of the wood particles and added adhesives (Zuber *et al.* 2020a). Based on the thermal analysis results, a compression temperature of 200 °C is considered suitable for the fabrication of the particleboard in this study.

Analysis of Density Using Gravimetric Method

The gravimetric method is used to determine the density of particleboard samples, as density is a critical factor that is closely associated with its mechanical strength, durability, and dimensional stability. Table 3 shows the density values for alginate-lignin bonded *Rhizophora* spp. particleboards.

Table 3. Density of Alginate-lignin Bonded *Rhizophora* spp. Particleboard Based on Gravimetric Method

Sample	Density by Gravimetric Method (gcm^{-3})	Deviation vs Soft Tissue (%)	Deviation vs Water (%)
A_0	1.03	0.98	3
A_3	0.99	2.94	1
A_6	1.03	0.98	3
B_0	1.16	13.7	16
B_3	1.15	12.7	15
B_6	1.06	3.92	6
C_0	0.95	6.86	5
C_3	1.01	0.98	1
C_6	1.01	0.98	1
Soft tissue (Noblet *et al.* 2018)	1.02	-	-
Water (Almalki *et al.* 2024)	1.00	-	-

Table 3 shows that the densities of the samples range from 0.95 to 1.16 gcm^{-3}. Sample B_0 with a particle size of 105 to 210 μm and 0% adhesive had the highest density, 1.16 gcm^{-3}, whereas sample C_0 with a particle size of 211 to 500 μm and 0% adhesive had the lowest density, 0.95 gcm^{-3}. Overall, the results showed good agreement for the fabrication of tissue-equivalent phantoms because the measured densities were close to the density of water, 1.0 gcm^{-3}. However, the density values of sample B_0 and B_3 differed considerably from the density of water. Both of these samples had a particle size of 105 to 210 μm and 0% and 3% adhesives, respectively.

The descriptive trend analysis of percentage deviation demonstrated that the particleboards with densities of approximately 1.03 gcm^{-3} and 1.01 gcm^{-3} exhibited superior radiological equivalence to soft tissue, as indicated by the lowest deviation value of 0.98% observed in sample A_0, A_6, C_3, and C_6. In contrast, the highest density sample, 1.16 gcm^{-3} showed a substantially greater deviation from soft tissue, reaching 13.7%, indicating poorer tissue equivalence. Regarding water equivalence, particleboards with densities around 0.99 gcm^{-3} and 1.01 gcm^{-3} demonstrated improved similarity, reflected by the minimum deviation value of 1% recorded in samples A_3, C_3, and C_6. Kruskal-Wallis test indicated that were statistically significant differences of particleboard density among particle size of *Rhizophora* spp. powder groups (0 to 104 μm, 105 to 210 μm, 211 to 500 μm) x^2= 19.651, df = 2, N = 27, p = 0.00 < 0.05. Therefore, post hoc pairwise comparisons were performed using Dunn's analysis with Bonferroni adjustment (p = 0.00). The results showed that the medium particle size, 105 to 210 μm had statistically significant difference between large, 211 to 500 μm (p = 0.00) and small, 0 to 104 μm (p = 0.013). However, there was no significant difference between large, 211 to 500 μm and small particle size, 0 to 104 μm (p = 0.39). Since the Kruskal-Wallis test indicated no significant differences of particleboard density among the adhesive formulation groups (0%, 3%, 6%) x^2= 0.603, df = 2, N = 27, p = 0.74 > 0.05, post hoc pairwise comparisons were not conducted.

According to previous study (Samson *et al.* 2023a,b), solid water has a density of 1.04 gcm^{-3}, soft tissue is roughly 1.03 gcm^{-3}, and water has a density of 1.0 gcm^{-3}. Density has an important impact on the attenuation of ionizing radiation in materials. To attain tissue equivalency, phantom materials should preferably have a mass density of 1.0 gcm^{-3}, as the density of water closely resembles that of human soft tissue (Zuber *et al.* 2020a,b). This alignment is particularly important, as the composition of water closely resembles that of human soft tissue, establishing it as a reference standard in radiological research (Büyükyıldız *et al.* 2024; Zuber *et al.* 2024). Therefore, the samples should possess densities closely matching those of water and soft tissue to ensure their suitability as phantom materials for medical physics applications. Overall, these findings suggest that particleboard densities in the range of approximately 1.01 to 1.03 gcm^{-3} provide the most favorable radiological matching soft tissue, while densities near 0.99 to 1.01 gcm^{-3} better approximate water. Consequently, these ranges are considered suitable for phantom fabrication due to their relevant radiological equivalence for diagnostic imaging application.

Analysis of Thickness Swelling and Water Absorption

Sodium alginate has natural adhesive qualities and is a hydrophilic substance (Akbar *et al.* 2023). Therefore, thickness swelling and water absorption tests are crucial to evaluate its performance for fabrication of tissue-equivalent phantom. The thickness swelling and water absorption values are recorded in Table 4.

Table 4. Thickness Swelling and Water Absorption of Alginate-Lignin Bonded *Rhizophora* spp. Particleboard

Sample	Thickness Swelling (%) ± Standard Deviation		Water Absorption (%) ± Standard Deviation	
A_0	18.75	0.48	38.50	0.16
A_3	18.76	1.47	42.03	0.00
A_6	18.67	0.92	38.02	0.43
B_0	39.46	1.77	41.79	0.42
B_3	35.23	0.53	50.76	0.00
B_6	34.23	0.95	70.45	0.00
C_0	48.37	1.52	76.13	1.26
C_3	46.84	1.41	61.20	0.47
C_6	41.58	0.81	71.03	0.00

Based on Table 4, sample C_0 with a particle size of 211 to 500 μm and 0% adhesive had the highest value of thickness swelling and water absorption, whereas sample A_6 with a particle size of 0 to 104 μm and 6% adhesive had the lowest value of thickness swelling. Although sample A_6 exhibited the lowest value of thickness swelling, it however did not fulfill the minimum requirement according to Japanese Industrial Standard, JIS A 5908

(JIS A 5908 2003), which establishes a 12% limit for the thickness swelling. Consequently, none of the samples satisfied this requirement, owing to the presence of *Rhizophora* spp., which contributed to increase water penetration due to their hydrophilic nature. In addition, the water absorption behavior of natural fibers is influenced by the presence of free hydroxyl groups in cellulose and hemicellulose, which are readily accessible to water molecules (Abdul Khalil *et al.* 2011). For future applications, smaller particle sizes are recommended to fulfill this requirement, as previous study (Engehausen *et al.* 2025) has shown that increasing particle size leads to higher TS and WA due to greater void formation, weaker interparticle bonding and enhanced water penetration. Thus, thickness swelling can adversely influence the mechanical integrity and dimensional stability of wood composite boards (Magalh *et al.* 2021). The results demonstrate that a smaller particle size is associated with a decrease in thickness swelling and water absorption percentages. It is possible that the smaller void in the particles allowed the natural adhesive molecule to settle within the void, whereas a larger particle size increased their capillary effect and hygroscopic qualities (Zuber *et al.* 2020b).

The Kruskal-Wallis test indicated that were statistically significant differences of thickness swelling among particle size of *Rhizophora* spp. powder groups (0 to 104 µm, 105 to 210 µm, 211 to 500 µm) x^2= 22.861, df = 2, N = 27, p = 0.00 < 0.05. Therefore, post hoc pairwise comparisons were performed using Dunn's analysis with Bonferroni adjustment (p = 0.00). The results showed that the small particle size, 0 to 104 µm had statistically significant difference between medium (p = 0.045) and large (p = 0.00). However, there was no significant difference between medium, 105 to 210 µm and large particle size, 211 to 500 µm (p = 0.057). Since the Kruskal-Wallis test indicated no significant differences of thickness swelling among the adhesive formulation groups (0%, 3%, 6%) x^2= 1.104, df = 2, N = 27, p = 0.576 > 0.05, post hoc pairwise comparisons were not conducted.

The Kruskal-Wallis test indicated that were statistically significant differences of water absorption among particle size of *Rhizophora* spp. powder groups (0 to 104 µm, 105 to 210 µm, 211 to 500 µm) x^2= 19.123, df = 2, N = 27, p = 0.00 < 0.05. Therefore, post hoc pairwise comparisons were performed using Dunn's analysis with Bonferroni adjustment (p = 0.00). The results showed that the small particle size, 0-104 µm had statistically significant difference between medium, 105 to 210 µm (p = 0.032) and large, 211 to 500 µm (p = 0.00). However, no significant difference between medium, 105 to 210 µm and large particle size, 211 to 500 µm (p = 0.217). Since the Kruskal-Wallis test indicated no significant differences of water absorption among the adhesive formulation groups (0%, 3%, 6%) x^2= 0.382, df = 2, N = 27, p = 0.826 > 0.05, post hoc pairwise comparisons were not conducted.

Morphological Analysis of Particleboards

The morphology images of alginate-lignin as natural-based adhesive bonded *Rhizophora* spp. particleboards were analyzed using FESEM at different magnification sizes based on Fig. 3. The morphology images of 0%, 3%, and 6% of sodium alginate and lignin adhesive bonded *Rhizophora* spp. were obtained at 1000×, 2000×, and 4000× magnification.

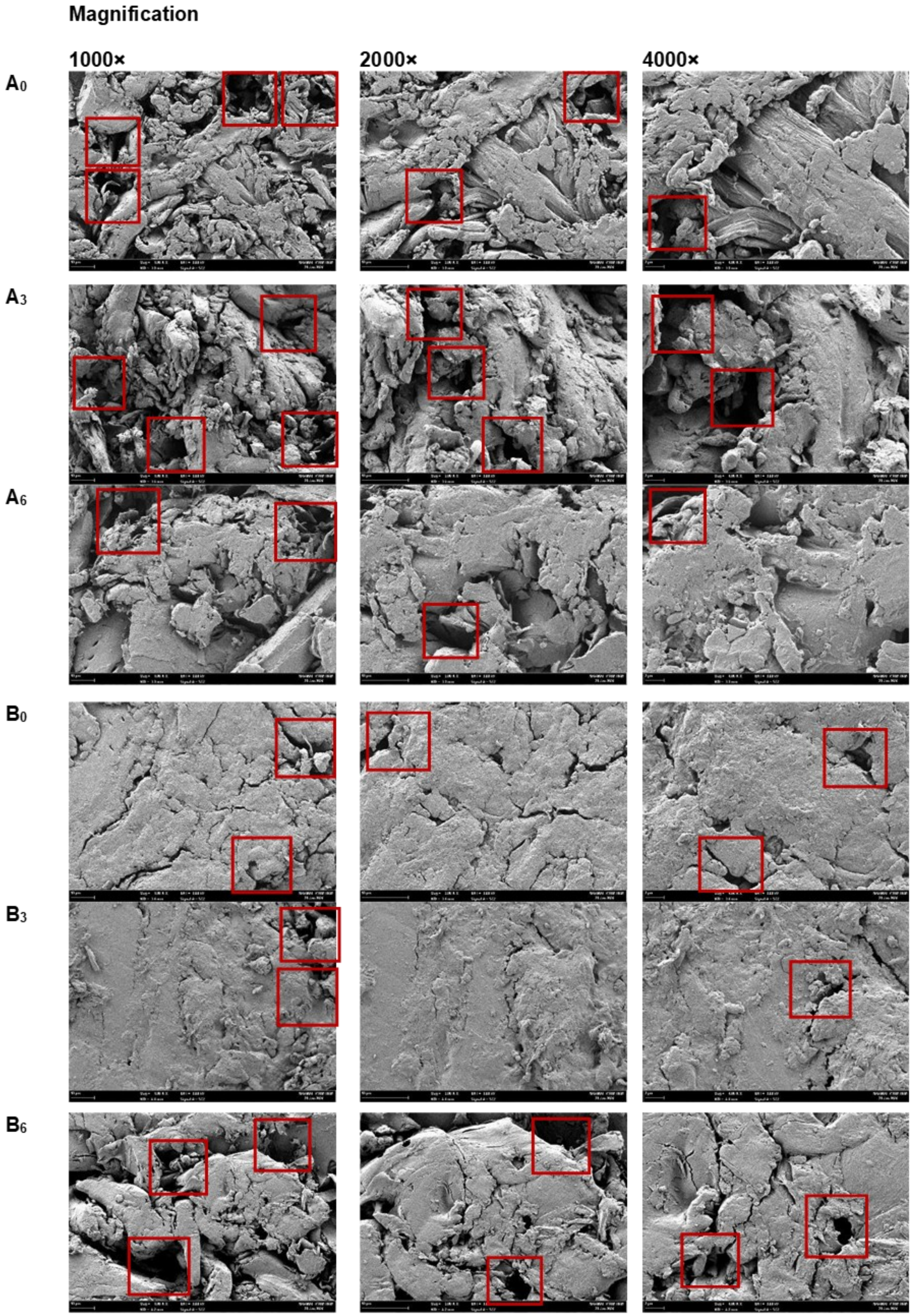
Magnification
1000×
2000×
4000×
A_0
A_3
A_6
B_0
B_3
B_6

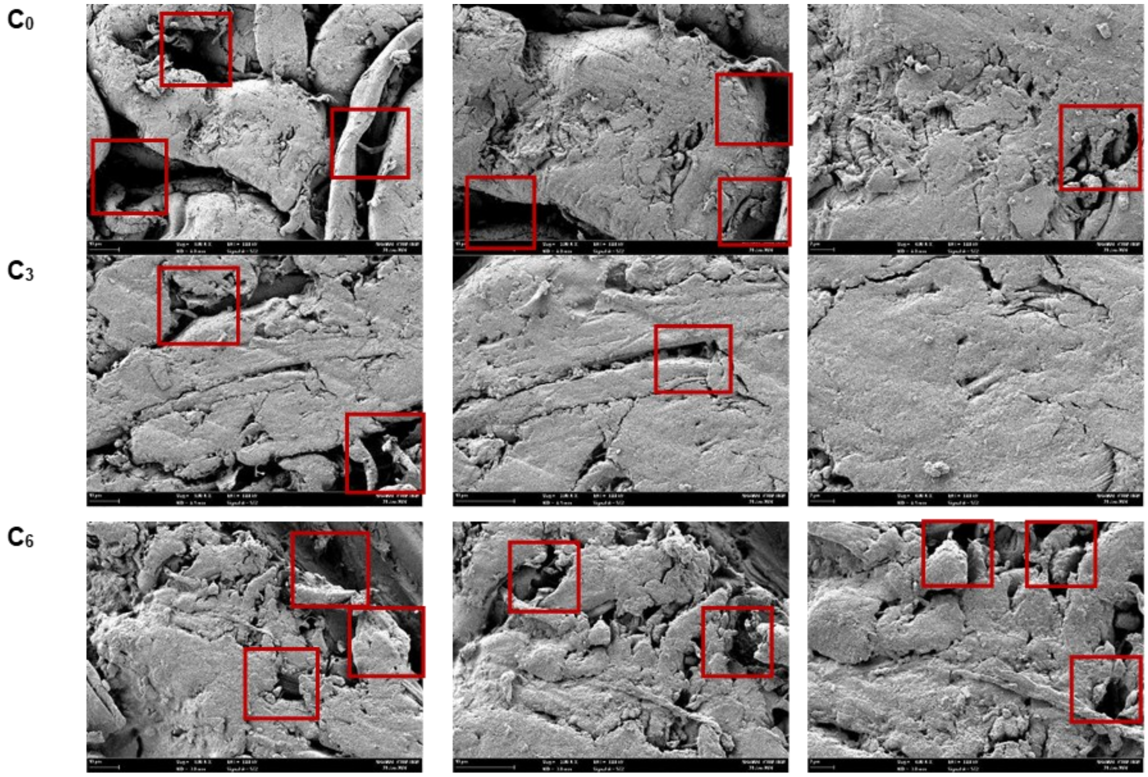

Fig. 3. Morphology of alginate-lignin bonded *Rhizophora* spp.; Particleboards at different magnification sizes of 1000×, 2000×, and 4000×; the red box highlights the region in which void spaces are present
A =0 to 104 µm, B =105 to 210 µm, C =211 to 500 µm particle size ranges. 0 =0% soy flour & lignin, 3 =2.5% sodium alginate & 0.5% lignin, 6 =5% sodium alginate & 1% lignin.

Based on Fig. 3, all samples of particleboard presented voids or empty spaces within the structure. However, 0% adhesive-bonded *Rhizophora* spp. particleboard with different particle sizes, A_0, B_0, and C_0 demonstrated a substantially greater presence of voids. As presented in Table 4, both TS and WA values decreased with decreasing particle size in the binderless particleboards. Sample C_0 exhibited a greater presence of voids compared to samples A_0 and B_0. The larger and more irregular void structure in C_0 is expected to have facilitated enhanced water penetration into the particleboard matrix, resulting in higher TS and WA values. This behavior can be attributed to the formation of micro-channels, which facilitate moisture transport and enable water diffusion through surface and internal pores. In addition, factors such as porosity, void content, lumen size, and fibre-matrix interfacial adhesion also substantially influence water absorption behavior of the composite. It has been widely reported that natural fibre-reinforced polymer composites exhibit high water absorption due to their inherent porosity and the presence of voids within the structure (Abdul Khalil *et al.* 2011).

In general, the amount of empty space in particleboard decreases as the adhesive content increases. The TS values showed a decreasing trend as the adhesive content increased. However, for WA, only particle size A, 0 to 104 µm, exhibited a reduction with increasing adhesive content, which can be attributed to its more uniform particle packing and improved interparticle contact. The presence of void spaces between the lumen and holes among the *Rhizophora* spp. particles contributed to the non-homogeneous distribution of the particles and a reduction in compactness of the binderless particleboards.

The appearance of voids showed that there were holes in specific particleboard parts, which led to a high absorption of water (Samson *et al.* 2020). According to a previous study (Yusof *et al.* 2017; Zuber *et al.* 2021a), when compared to the binderless sample, the empty spaces between the molecules were smaller, providing the sample with a smoother appearance. This is attributed to the hot-pressing process, which promotes the condensation of wood particles and binder, resulting in improved bonding between them. A reduction in compactness and binding is indicated by the large number of empty spaces found, which could have an impact on the mechanical and physical characteristics of the particleboard (Yusof *et al.* 2017; Zuber *et al.* 2020a). Overall, the findings suggest that particle size A, 0 to 104 µm is more suitable for tissue-equivalent phantom fabrication because higher adhesive content contributed to the reduction of void spaces within this particle size group.

Elemental Composition of Particleboards

The elemental composition of alginate-lignin bonded *Rhizophora* spp. particleboards was analyzed using EDX attached to a FESEM. Table 5 shows the weight percentage of the elemental composition for the particleboards. Figure 4 demonstrates the EDX spectrum for the samples.

Table 5. Weight Percentage of Elemental Composition for Alginate-lignin bonded *Rhizophora* spp. Particleboards

Sample	Weight Fraction of Elements (%)			
	C	O	Na	Ca
A_0	52.8	46.6	-	0.6
A_3	51.3	46.5	0.8	1.3
A_6	51.0	44.9	2.8	1.3
B_0	51.7	46.3	0.9	1.1
B_3	52.4	46.3	1.3	-
B_6	53.0	45.4	0.8	0.8
C_0	52.2	47.8	-	-
C_3	53.2	45.5	1.3	-
C_6	51.2	46.9	1.6	0.3

Based on the results, carbon constituted the highest weight percentage of elemental composition for all the samples, with oxygen being the second most abundant element. This is because the two main natural elements found in wood particles are carbon and oxygen. Carbon and oxygen constitute the majority of the main components of wood, which are lignin, cellulose, and hemicellulose (Siddique *et al.* 2024). In the elemental composition, calcium exhibited the lowest weight percentage and was not detected in samples B_3, C_0, and C_3. The presence of sodium alginate as a binder is linked to the detected sodium in the samples. In general, the weight percentage of sodium in the elemental composition increased with increasing adhesive content. Previous research reported the elemental composition of soft tissue is primarily composed of oxygen (63.0238%), followed by carbon (23.219%) being the second most abundant element and calcium (0.023%) being present in smaller amounts (Ogunsina *et al.* 2023). Therefore, the presence of oxygen, carbon, and calcium within the samples supports the suitability of the materials for the development of tissue-equivalent phantoms.

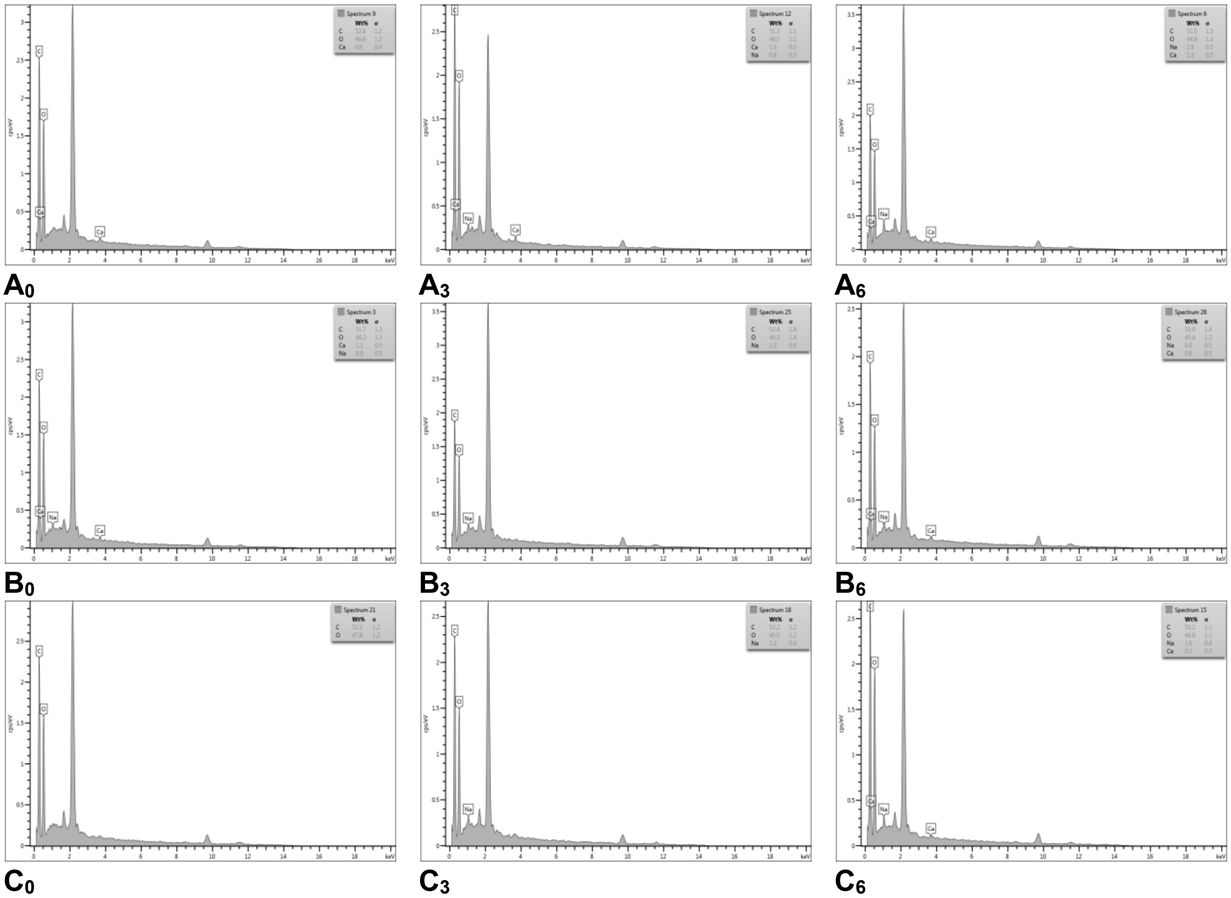

Fig. 4. Energy dispersive X-ray spectrum for alginate-lignin bonded *Rhizophora* spp. particleboards
A =0 to 104 µm, B =105 to 210 µm, C =211 to 500 µm particle size ranges. 0 =0% soy flour & lignin, 3 =2.5% sodium alginate & 0.5% lignin, 6 =5% sodium alginate & 1% lignin

Analysis of Effective Atomic Number, Z_{eff}

In radiation research, photon interaction characteristics, such as the effective atomic number, Z_{eff}, are crucial for characterizing how photons interact with a target material. These factors are especially crucial when assessing materials that are designed to be used as phantoms (Zuber *et al.* 2021c). Therefore, the effective atomic number of alginate-lignin as natural-based adhesive bonded *Rhizophora* spp. particleboards were calculated using the weight percentage of elemental composition that were obtained from EDX analysis. Table 6 shows the atomic fraction and effective atomic number, Z_{eff} of the elemental composition for each sample.

Based on the results, the effective atomic number, Z_{eff}, of the samples range from 6.98 to 7.39. Sample A_6 with a particle size of 0 to 104 µm and 6% adhesive had the highest Z_{eff} value, 7.39, whereas sample C_0 with a particle size of 211 to 500 µm and 0% adhesive had the lowest Z_{eff} value, 6.98. The descriptive trend analysis of Z_{eff} demonstrated that increasing the adhesive composition and reducing particle size enhanced the radiological equivalence of the fabricated particleboards toward soft tissue and water. Sample C_0, fabricated without adhesive, exhibited the lowest Z_{eff} value of 6.98 and the highest percentage deviations from soft tissue, 6.18% and water, 5.93%, indicating lower tissue equivalence. In contrast, the incorporation of lignin and sodium alginate increased the Z_{eff} values while progressively reducing the deviation percentages. Sample A_6 exhibited the highest Z_{eff} value of 7.39, with the lowest deviations from soft tissue, 0.67% and water, 0.40%, indicating the closest radiological equivalence to the reference materials. Since the Kruskal-Wallis test indicated no significant differences of Z_{eff} among the particle size of *Rhizophora* spp. powder groups (0 to 104 µm, 105 to 210 µm, 211 to 500 µm) x^2= 3.693, df = 2, N = 27, p = 0.158 > 0.05, post hoc pairwise comparisons were not conducted. The Kruskal-Wallis test indicated that were statistically significant differences of Z_{eff} among adhesive formulation groups (0%, 3%, 6%) x^2= 6.572, df = 2, N = 27, p = 0.037 < 0.05. Therefore, post hoc pairwise comparisons were performed using Dunn's analysis with Bonferroni adjustment (p = 0.037). The results showed that the 0% adhesive formulation exhibited no significant difference between 3% (p = 0.98) and 6% (p = 0.356). However, there was a statistically significant difference between 3% and 6% adhesive formulation (p = 0.033).

Table 6. Atomic Fraction and Effective Atomic Number, Z_{eff} of the Elements in Alginate-lignin Bonded *Rhizophora* spp. Particleboards

Sample	Atomic Fraction of Elements (%)				Z_{eff}	Deviation vs Soft Tissue (%)	Deviation vs Water (%)
	C	O	Na	Ca			
A_0	60.0	39.7	-	0.205	7.11	4.44	4.17
A_3	59.0	40.1	0.480	0.448	7.32	1.61	1.35
A_6	58.9	38.9	1.69	0.451	7.39	0.67	0.40
B_0	59.3	39.8	0.538	0.378	7.27	2.28	2.02
B_3	59.7	39.5	0.772	-	7.02	5.65	5.39
B_6	60.4	38.8	0.476	0.274	7.18	3.49	3.23
C_0	59.3	40.7	-	-	6.98	6.18	5.93
C_3	60.5	38.8	0.771	-	7.01	5.78	5.53
C_6	58.6	40.3	0.956	0.103	7.13	4.17	3.91
Soft tissue (Noblet *et al.* 2018)					7.44	-	-
Water (Samson *et al.* 2021)					7.42	-	-

In a variety of medical applications (Abady *et al.* 2023), the effective atomic number, Z_{eff}, is a useful parameter to determine the radiation response of composite materials. It is an essential measure for evaluating photon absorption and scattering capabilities of composite materials along with tissue equivalence. According to previous studies (Samson *et al.* 2021; Vrbaški *et al.* 2023), the effective atomic number, Z_{eff}, of water has been reported as 7.42 and 7.44, respectively. Water is known to be a good medium to simulate the human body because of its characteristics. In radiation and dosimetry studies, water also shows great measurement for radiation absorption and scattering (Zuber *et al.* 2021c). Sample A_6 exhibited the highest sodium content, 1,69% due to its higher adhesive composition and consequently produced the highest effective atomic number, Z_{eff} of 7.39. This behavior can be attributed to atomic number of sodium, Z=11, which possesses a higher atomic number than the primary constituents of lignocellulosic biomass, namely carbon, Z=6 and oxygen, Z=8. As the atomic number is one of the most significant parameters influencing the radiation interaction characteristics of a material, the effective atomic number, Z_{eff}, can be used to characterize the radiological properties of phantom materials (Rezaeian *et al.* 2023). Therefore, sample A_6 was considered the most suitable candidate for phantom fabrication due to its greater similarity to the effective atomic number, Z_{eff} of human soft tissue and water.

CONCLUSIONS

1. *Rhizophora* spp. particleboard bonded with sodium alginate and lignin demonstrated promising potential for tissue-equivalent phantom applications. Sample A_6, with 0 to 104 µm and 6% adhesive content, exhibited density and effective atomic number Z_{eff} comparable to those of water and soft tissue, with relatively low thickness swelling and water absorption values.
2. The density values of particleboards using the gravimetric method demonstrated good agreement for the fabrication of tissue-equivalent phantoms because they were close to the density of water.
3. The smallest particle size and the highest adhesive content exhibited the lowest thickness swelling and water absorption values, although the results did not fully comply with the standard requirements.
4. The scanning electron microscope (SEM) images indicated that the presence of void spaces within the particleboard structure decreased when the adhesive content of the particleboard increased.
5. The energy-dispersive X-ray (EDX) analysis demonstrated that the weight percentage of sodium in elemental composition improved as the adhesive quantity increased because sodium alginate was used as a binding agent in particleboard fabrication.
6. The effective atomic number, Z_{eff} of particleboards, was calculated and demonstrated good agreement for the fabrication of tissue-equivalent phantoms because they were close to the effective atomic number, Z_{eff} of water.

ACKNOWLEDGMENTS

The authors would like to acknowledge the Centre for Diagnostic, Therapeutic and Investigative Studies, Faculty of Health Sciences, Universiti Kebangsaan Malaysia for allowing the research of this study to be conducted accordingly. This work was funded by the Fundamental Research Grant Scheme (FRGS/1/2024/STG07/UKM/02/4) from the Ministry of Higher Education (MOHE), Malaysia. This work was also supported by Geran Galakan Penyelidik Muda (GGPM-2023-027), Universiti Kebangsaan Malaysia.

USE OF GENERATIVE AI

ChatGPT (GPT-5) was employed primarily for rephrasing sentences and elaboration to enhance clarity and readability, and for grammar checking to ensure linguistic accuracy in academic and professional writing.

REFERENCES CITED

Abady, R. S., Sharaf, J. M., Imran, M. M., Saleh, H. H., and Alkhateeb, S. B. (2023). "Study of effective atomic number, mass energy absorption coefficient and absorbed dose rate in human organ and tissue substitutes," *Jordan J. Phys.* 16, 271-284. https://doi.org/10.47011/16.3.3

Abdul Khalil, H. P. S., Jawaid, M., and Abu Bakar, A. (2011). "Woven hybrid composites: Water absorption and thickness swelling behaviours," *BioResources* 6(2), 1043-1052. https://doi.org/10.15376/biores.6.2.1043-1052

Abuarra, A., Bauk, S., Hashim, R., Kandaiya, S., and Tousi, E. T. (2014). "Microstructure examination, elemental composition analysis of gum arabic bonded *Rhizophora* spp. particleboards and their potential as tissue equivalent material," *Int. J. Chem. Environ. Biol. Sci.* 2, 71-75. https://doi.org/10.1016/j.matdes.2014.03.032

Ahluwalia, V.K. (2023). "Thermogravimetric analysis," in: *Instrumental Methods of Chemical Analysis*, Springer, Cham., pp. 81-82. https://doi.org/10.1007/978-3-031-38355-7_11

Akbar, M., Yaqoob, A., Ahmad, A., and Luque, R., (2023). "Sodium alginate: An overview," in: *Sodium Alginate-Based Nanomaterials for Wastewater Treatment*, Elsevier, Amsterdam, Netherlands, pp. 1–17. https://doi.org/10.1016/B978-0-12-823551-5.00012-4

Ali, S., Rani, A., Dar, M. A., Qaisrani, M. M., Noman, M., Yoganathan, K., Asad, M., Berhanu, A., Barwant, M., and Zhu, D. (2024). "Recent advances in characterization and valorization of lignin and its value-added products: Challenges and future perspectives," *Biomass* 4, 947-977. https://doi.org/10.3390/biomass4030053

Almalki, H., Marashdeh, M. W., Alsuhybani, M., and Almurayshid, M. (2024). "Evaluation of radiation attenuation properties of breast equivalent phantom material made of gelatin material in mammographic X-ray energies," *J. Radiat. Res. Appl. Sci.* 17, article 100817. https://doi.org/10.1016/j.jrras.2024.100817

Badita, C. R., Aranghel, D., Burducea, C., and Mereuta, P. (2020). "Characterization of sodium alginate-based films," *Rom. J. Phys.* 65, article 602. https://rjp.nipne.ro//2020_65_1-2/RomJPhys.65.602.pdf

Bello, O. M., Nor, N. M., and Hassan, W. M. S. W. (2022). "Characterization of the urethane-based tissue equivalent substitute for phantom construction: Model molding, XCOM and MCNPX Studies," *Int. J. Adv. Sci. Eng. Inf. Technol.* 12, 298-305. https://doi.org/10.18517/ijaseit.12.1.13815

Bublex, A., Montalibet, A., Massot, B., and Gehin, C. (2025). "Review of phantoms for mimicking the electrical properties and mechanical strength of living tissue," *IRBM* 46(5), article 100904. https://doi.org/10.1016/j.irbm.2025.100904

Büyükyıldız, M., Kaur, P., Thakur, S., and Atlı, R. (2024). "Study of phantom materials close to 1 keV photon energy for radiation applications," *Radiat. Phys. Chem.* 215, article 111375. https://doi.org/10.1016/j.radphyschem.2023.111375

Engehausen, N., Benthien, J. T., and Lüdtke, J. (2025). "Investigation on the influence of particle size and surface-specific adhesive amount on mechanical properties and sorption behavior of particleboard," *Eur. J. Wood Prod.* 83, 123. https://doi.org/10.1007/s00107-025-02275-3

Frent, O. D., Vicas, L. G., Duteanu, N., Morgovan, C. M., Jurca, T., Pallag, A., Muresan, M. E., Filip, S. M., Lucaciu, R. L., and Marian, E. (2022). "Sodium alginate—Natural microencapsulation material of polymeric microparticles," *Int. J. Mol. Sci.* 23(20),

article 12108. https://doi.org/10.3390/ijms232012108
Hoan, N. X., Anh, L. T. H., Ha, H. T., and Cuong, D. X. (2023). "Antioxidant activities, anticancer activity, physico-chemistry characteristics, and acute toxicity of alginate/ lignin polymer," *Molecules* 28(13), article 5181. https://doi.org/10.3390/molecules28135181
JIS A 5908 (2003). "Particleboards: Determination of physical and mechanical properties of the particleboard," Japanese Industrial Standard, Tokyo, Japan.
Jusufbegović, M., Pandžić, A., Šehić, A., Jašić, R., Julardžija, F., Vegar-Zubović, S., and Beganović, A. (2022). "Computed tomography tissue equivalence of 3D printing materials," *Radiography* 28, 788-792. https://doi.org/10.1016/j.radi.2022.02.008
Karthikeyan, S., and Samuel, E. J. J. (2022). "Studies on the tissue and water equivalence of some 3D printing materials and dosimeters," *Radiat. Phys. Chem.* 198, article 110259. https://doi.org/10.1016/j.radphyschem.2022.110259
Khallouqi, A., Halimi, A., El Rhazouani, O., Mesradi, M. R., El Mansouri, K., and Sekkat, H. (2024). "Comparing tissue-equivalent properties of polyester and epoxy resins with PMMA material using Gate/Geant4 simulation toolkit," *Radiat. Phys. Chem.* 220, article 111702. https://doi.org/10.1016/j.radphyschem.2024.111702
Khallouqi, A., Halimi, A., and El, O. (2025). "Cost-effective pediatric head phantom for computed tomography dosimetry and its evaluation using pencil ion chamber and OSLD," *Radiat. Phys. Chem.* 237, article 113040. https://doi.org/10.1016/j.radphyschem.2025.113040
Linan, L. Z., Fakhouri, F. M., Nogueira, G. F., Zoppe, J., and Velasco, J. I. (2024). "Benefits of incorporating lignin into starch-based films: A brief review," *Polymer* 16(16), article 2285. https://doi.org/10.3390/polym16162285
Luan, Q. Y., Wang, Y. S., Chen, Y., and Chen, H. H. (2025). "Review on improvement of physicochemical properties of sodium alginate-based edible films," *J. Food Sci.* 90(2), article e70016. https://doi.org/10.1111/1750-3841.70016
Magalh, R., Nogueira, B., Costa, S., Paiva, N., Ferra, M., Magalh, D., Martins, J., and Carvalho, L. H. (2021). "Effect of panel moisture content on internal bond strength and thickness swelling of medium density fiberboard," *Polymers* 13, article 114. https://doi.org/10.3390/polym13010114
Marashdeh, M. W., Hashim, R., Tajuuddin, A. A., Bauk, S., and Sulaiman, O. (2011). "Effect of particle size on the characterization of binderless particleboard made from *Rhizophora* Spp. mangrove wood for use as phantom material," *BioResources* 6(4), 4028-4044. https://doi.org/10.15376/biores.6.4.4028-4044
Maulana, M. I., Adly, M., Lubis, R., Febrianto, F., Hua, L. S., Iswanto, A. H., Antov, P., Kristak, L., Mardawati, E., and Sari, R. K. (2022). "Environmentally friendly starch-based adhesives for bonding high-performance wood composites: A review," *Forests* 13(10), article 1614. https://doi.org/10.3390/f13101614
Nisa, K. A., Anam, C., Alkian, I., Naufal, A., and Sutanto, H. (2025). "Design and fabrication of paediatric chest phantom using polymethyl methacrylate-polyurethane foam for pneumonia imaging evaluation," *Radiation Physics and Chemistry* 232, article 112610. https://doi.org/10.1016/j.radphyschem.2025.112610
Noblet, C., Delpon, G., Supiot, S., Potiron, V., Paris, F., and Chiavassa, S. (2018). "A new tissue segmentation method to calculate 3D dose in small animal radiation therapy," *Radiat Oncol* 13, article 32. https://doi.org/10.1186/s13014-018-0971-8
Ogunsina, S. A., Balogun, F. A., Saidu, A., Umakha, M., and Sule, A. (2023). "Suitability of different materials as human tissue simulating materials in Co-60

radiation energy beam," *UMYU Sci.* 2, 145-149. https://doi.org/10.56919/usci.2324.018

Peijs, T., Kirschbaum, R., and Lemstra, P. J. (2022). "Chapter 5: A critical review of carbon fiber and related products from an industrial perspective," *Adv. Ind. Eng. Polym. Res.* 5, 90-106. https://doi.org/10.1016/j.aiepr.2022.03.008

Qiu, H., Nazarenus, J., Egeler, B., Thode, T., Osman, F., Osmonov, D., Bahr, J., Kaps, S., Siebert, F. A., Koch, R., *et al.* (2024). "Hydrogel system with independent tailoring of mechanics, CT, and US contrasts for affordable medical phantoms," *ACS Mater. Lett.* 6(10), 4847-4853. https://doi.org/10.1021/acsmaterialslett.4c01660

Rezaeian, P., Kashian, S., and Mehrara, R. (2023). "Investigation of the effective atomic number dependency on kinetic energy using collision stopping powers for electrons, protons, alpha, and carbon particles," *Sci. Rep.* 13, article 3573. https://doi.org/10.1038/s41598-023-30491-5

Samson, D. O., Mat Jafri, M. Z., Hashim, R., Sulaiman, O., Aziz, M. Z. A., Yusof, M. F. M., and Shukri, A. (2020a). "*Rhizophora* spp. particleboards incorporating defatted soy flour bonded with NaOH/IA-PAE: Towards a water equivalent phantom material," *Radiat. Phys. Chem.* 176, article 109057. https://doi.org/10.1016/j.radphyschem.2020.109057

Samson, D. O., Shukri, A., Jafri, M. Z. M., Hashim, R., Aziz, M. Z. A., and Yusof, M. F. M. (2020b). "Fabrication and dosimetric characterization of novel bio-based tissue substitute phantom materials," *Journal of Critical Review* 7, 862-872.

Samson, D. O., Shukri, A., Aziz Hashikin, N. A., Zuber, S. H., Addo Buba, A. D., Abdul Aziz, M. Z., Hashim, R., Mohd Yusof, M. F., Gemanam, S. J., and Samson, P. A. (2023a). "Performance of natural product-based materials as adhesives in the fabrication of mangrove wood composites," *Heliyon* 9, article e13032. https://doi.org/10.1016/j.heliyon.2023.e13032

Samson, D. O., Shukri, A., Hashikin, N. A. A., Zuber, S. H., Aziz, M. Z. A., Hashim, R., Yusof, M. F. M., Rabaiee, N. A., and Gemanam, S. J. (2023b). "Dosimetric characterization of DSF/NaOH/IA-PAE/*R*. spp. phantom material for radiation therapy," *Polymers (Basel)* 15(1), article 244. https://doi.org/10.3390/polym15010244

Samson, D. O., Shukri, A., Mat Jafri, M. Z., Hashim, R., Sulaiman, O., Abdul Aziz, M. Z., and Mohd Yusof, M. F. (2021). "Characterization of *Rhizophora* spp. particleboards with soy protein isolate modified with NaOH/IA-PAE adhesive for use as phantom material at photon energies of 16.59–25.26 keV," *Nucl. Eng. Technol.* 53, 216-233. https://doi.org/10.1016/j.net.2020.06.005

Samson, D. O., Zuber, S. H., Shukri, A., Aziz, M. Z. A., Biodun, A. D., Fadzil, M. S. A., Yahya, N. A., and Buba, A. D. A. (2025). "New alternative equivalent phantom materials developed for radiotherapy applications," *J. Phys. Conf. Ser.* 2944, article 012012. https://doi.org/10.1088/1742-6596/2944/1/012012

Shah, S. W. A., Xu, Q., Ullah, M. W., Zahoor, Sethupathy, S., Morales, G. M., Sun, J., and Zhu, D. (2023). "Lignin-based additive materials: A review of current status, challenges, and future perspectives," *Addit. Manuf.* 74, article 103711. https://doi.org/10.1016/j.addma.2023.103711

Siddique, M., Soomro, S. A., and Aziz, S. (2024). "Characterization and optimization of lignin extraction from lignocellulosic biomass *via* green nanocatalyst," *Biomass Convers. Biorefinery* 14, 28523-28531. https://doi.org/10.1007/s13399-022-03598-4

Slobozeanu, A. E., Bejan, S. E., Tudor, I. A., Mocioiu, A., Motoc, A. M., Romerosanchez, M. D., Botan, M., Catalin, C. G., Madalina, C. L., Piticescu, R. R., and Predescu, C. (2021). "A review on differential scanning calorimetry as a tool for thermal assessment of nanostructured coatings," *Manufacturing Rev.* 8, 1-15. https://doi.org/10.1051/mfreview/2020038

Tousi, E. T., Hashim, R., Bauk, S., and Jaafar, M. S. (2015). "Characterization of the *Rhizophora* particleboard as a tissue-equivalent phantom material bonded with bio-based adhesive," *Maderas. Ciencia. Tecnol.* 17, 305-318. https://doi.org/10.4067/S0718-221X2015005000029

Tousi, E. T., Hashim, R., Bauk, S., Jaafar, M. S., Abuarra, A. M. H., and Ababneh, B. (2014). "Some properties of particleboards produced from *Rhizophora* spp. as a tissue-equivalent phantom material bonded with *Eremurus* spp. Meas," *J. Int. Meas. Confed.* 54, 14-21. https://doi.org/10.1016/j.measurement.2014.04.004

Vrbaški, S., Arana Peña, L. M., Brombal, L., Donato, S., Taibi, A., Contillo, A., and Longo, R. (2023). "Characterization of breast tissues in density and effective atomic number basis *via* spectral X-ray computed tomography," *Phys. Med. Biol.* 68, article 145019. https://doi.org/10.1088/1361-6560/acdbb6

Wegner, M., Gargioni, E., and Krause, D. (2023). "Classification of phantoms for medical imaging," *Procedia CIRP* 119, 1140-1145. https://doi.org/10.1016/j.procir.2023.03.154

Wu, W., Li, P., Huang, L., Wei, Y., Li, J., Zhang, L., and Jin, Y. (2023). "The role of lignin structure on cellulase adsorption and enzymatic hydrolysis," *Biomass (Switzerland)* 3, 96-107. https://doi.org/10.3390/biomass3010007

Yusof, M. F. M., Hashim, R., Tajuddin, A. A., Bauk, S., and Sulaiman, O. (2017). "Characterization of tannin-added *Rhizophora* spp. particleboards as phantom materials for photon beams," *Ind. Crops Prod.* 95, 467-474. https://doi.org/10.1016/j.indcrop.2016.10.057

Zuber, S. H., Hashikin, N. A. A., Yusof, M. F. M., and Hashim, R. (2020a). "Lignin and soy flour as adhesive materials in the fabrication of *Rhizophora* spp. particleboard for medical physics applications," *J. Adhes.* 98(5), 429-448. https://doi.org/10.1080/00218464.2020.1839430

Zuber, S. H., Hashikin, N. A. A., Yusof, M. F. M., and Hashim, R. (2020b). "Physical and mechanical properties of soy-lignin bonded *Rhizophora* spp. particleboard as a tissue-equivalent phantom material," *BioResources* 15(3), 5558-5576. https://doi.org/10.15376/biores.15.3.5558-5576

Zuber, S. H., Hashikin, N. A. A., Yusof, M. F. M., Aziz, M. Z. A., and Hashim, R. (2021a). "Influence of different percentages of binders on the physico-mechanical properties of *Rhizophora* spp. particleboard as natural-based tissue-equivalent phantom for radiation dosimetry applications," *Polymers (Basel)* 13(11), article 1868. https://doi.org/10.3390/polym13111868

Zuber, S. H., Hashikin, N. A. A., Yusof, M. F. M., Aziz, M. Z. A., and Hashim, R. (2021b). "Characterization of soy-lignin bonded *Rhizophora* spp. particleboard as substitute phantom material for radiation dosimetric studies – Investigation of CT number, mass attenuation coefficient and effective atomic number," *Appl. Radiat. Isot.* 170, article 109601. https://doi.org/10.1016/j.apradiso.2021.109601

Zuber, S. H., Hashikin, N. A. A., Yusof, M. F. M., Hashim, R., and Aziz, M. Z. A. (2021c). "Effective atomic number based on energy dispersive X-ray (EDX) analysis and carbon hydrogen nitrogen (CHN) analysis for phantom material in medical physics applications," *Malaysian J. Med. Heal. Sci.* 17, 116-121. http://mjmhsojs.upm.edu.my/index.php/mjmhs/article/view/474

Zuber, S. H., Abdul Hadi, M. F. R., Hashikin, N. A. A., Yusof, M. F. M., and Aziz, M. Z. A. (2024). "*Rhizophora*-based particleboard bonded with soy flour and lignin as potential phantom," *BioResources* 19(3), 5467-5482. https://doi.org/10.15376/biores.19.3.5467-5482

Article submitted: March 24, 2026; Peer review completed: May 3, 2026; Revised version received and accepted: June 13, 2026; Published: July 21, 2026.
DOI: 10.15376/biores.21.3.8444-8466